# Temperature-dependent magnetic second-harmonic generation from Fe nanostructures grown on vicinal W(110)

L. Carroll, J. P. Cunniffe, K. Fleischer, S. Ryan, and J. F. McGilp*
*School of Physics, Trinity College Dublin, Dublin 2, Republic of Ireland*
(Received 11 January 2011; revised manuscript received 7 March 2011; published 21 April 2011)

Temperature-dependent magnetic second-harmonic generation (MSHG) at normal incidence (NI) is used to determine magnetization curves from Au-capped ultrathin Fe nanostructures grown on a vicinal W(110) substrate. Aligned magnetic nanostructures grown on low-symmetry interfaces are generally inhomogeneous, with different magnetic species, such as terrace and step atoms, contributing to the overall magnetic response from the interfacial regions. A phenomenological model of NI MSHG intensity and contrast at magnetic interfaces of 1 m symmetry is used to extract the magnetization information. Two characteristic temperatures are identified for both 0.75 and 2.0 monolayers of Fe, and it is proposed that the increased sensitivity of SHG to step atoms, compared to linear optical techniques, allows the contribution of boundary atoms to the spin block response to be directly detected at lower temperatures. The behavior of boundary spins such as these is expected to be important for atomic-scale magnetic structures.

DOI: 10.1103/PhysRevB.83.134429 PACS number(s): 75.70.Ak, 75.70.Cn, 42.65.Ky

## I. INTRODUCTION

Magnetic nanostructures exhibit novel physical phenomena not observed in bulk magnetic systems.[1] The magnetic properties of these low-dimensional systems often depend sensitively on both the morphology and symmetry of the nanostructures and the substrate on which they are grown.[2] Magnetic nanostructures must be protected from the environment if they are to have a technological application, and this is often accomplished by capping the structure with a thin nonmagnetic layer. However, capping these structures with protective layers of nonmagnetic material may modify their magnetic properties,[3,4] making the characterization of the buried interfacial region of such a capped structure essential to understanding the underlying physics and materials science. Conventional surface techniques are insensitive to buried nanostructures, but a variety of optical techniques, with their larger penetration depth, can provide useful data. Photon-in–photon-out techniques ("epioptics"[5,6]), such as optical second-harmonic generation (SHG), which use symmetry to extract the optical response of the interface from the normally dominant bulk response, allow the buried interfacial structure of centrosymmetric materials to be probed through thin capping layers, and magnetic SHG (MSHG) extends this to magnetic interfaces. However, the vast majority of magnetic thin-film systems that have been studied so far are of high surface and interface symmetry,[7] because of the general complexity of the MSHG response and the often poor signal-to-noise ratio (SNR).[8] Lower symmetry systems, which may have multiple magnetic regions, have many tensor components that may contribute to the MSHG intensity, making interpretation particularly difficult. We have shown recently that normal incidence (NI) geometry, which drastically reduces the number of tensor components contributing to the signal, allows useful information to be extracted from the MSHG response of aligned magnetic nanostructures grown on low-symmetry interfaces.[9,10] Although NI geometry reduces the size of the SH response significantly, reasonable SNRs using unamplified fs pulses were obtained from submonolayer (ML) amounts of Fe deposited on a vicinal W(110) substrate and capped by 16 nm of Au.

MSHG measurements at 80 K of this well-known Fe nanostripe structure grown on W(110),[11–14] capped with Au,[15,16] allowed a hysteresis loop from 10-atom-wide Fe nanostripes to be detected.[10] The results for 30-atom-wide Fe nanostripes at 0.75 ML Fe coverage were of particular interest, as two loop components were clearly identified, leading to the suggestion that MSHG can distinguish the magnetic response of the terrace and the boundary (step and edge) Fe atoms in the nanostripes. For the 2 ML bilayer Fe structure, only a single interfacial component and loop could be reliably identified,[10] although close inspection revealed some evidence of a second component.

The smallest magnetic nanostructures are grown on the aligned atomic steps of vicinal substrates,[13,17] which typically show only 1 m symmetry in the SHG response from the surface or interface, with the single mirror plane orthogonal to the step.[18] This 1 m structure is particularly challenging, having ten allowed crystallographic tensor components that can contribute to the SHG signal, and up to eight additional magnetic tensor components, for an in-plane magnetic easy axis aligned with the 1 m mirror plane. However, normal or near-normal incidence SHG geometry simplifies the nonlinear response from such low-symmetry systems by excluding $z$-dependent tensor components. The MSHG intensity from a magnetic interface, within the electric dipole approximation, is given by

$$I(2\omega;\pm\boldsymbol{M}) \propto \left|\boldsymbol{\chi}^{\mathrm{eff}}_{\mathrm{even}}\boldsymbol{E}(\omega)\boldsymbol{E}(\omega) \pm \boldsymbol{\chi}^{\mathrm{eff}}_{\mathrm{odd}}\boldsymbol{M}\boldsymbol{E}(\omega)\boldsymbol{E}(\omega)\right|^2, \quad (1)$$

where $\boldsymbol{\chi}^{\mathrm{eff}}_{\mathrm{even}}$ is the effective third-rank crystallographic susceptibility tensor, $\boldsymbol{E}(\omega)$ is the input electric field vector, $\boldsymbol{\chi}^{\mathrm{eff}}_{\mathrm{odd}}$ is the effective fourth-rank axial magnetic susceptibility tensor, and $\boldsymbol{M}$ is the interface magnetization.[19] The combination of NI and the choice of azimuth removes any possible higher-order crystallographic quadrupolar contribution from the substrate or capping layer. SHG is known to be sensitive to strain,[20] and any magnetoelastic effects will appear in the *even* term.[21,22] Appropriate Fresnel and local-field factors[23] are included in the effective tensors, as NI geometry reduces these contributions to simple scaling factors. It has been

 

shown that, through a careful choice of sample alignment with respect to input polarization selection and the direction of applied magnetic field, it is possible to measure an NI MSHG intensity from 1 m magnetic interfaces containing just one contributory crystallographic tensor component (*even* with respect to reversal of the magnetization direction) and two magnetic (*odd*) tensor components.[24] It has been demonstrated that, with this geometry, the relative magnitude and relative phase of the *even* and *odd* components can be determined.[9]

Low-symmetry magnetic interfaces are inhomogeneous, containing two or more regions where the same magnetic species is found with a different number of magnetic and nonmagnetic nearest neighbors. Since the magnetic properties of an interface are known to depend sensitively on nearest-neighbor number and type,[12] a full description of NI MSHG from an inhomogeneous interface must account for the contributions made by components from the different regions. Fine tuning of the input polarization direction enhances the magnetic contribution to the NI SHG signal, resulting in a significant improvement in the SNR of hysteresis loops and magnetic contrast extracted from the measurements. The improved SNR allows the presence of different magnetic regions at the inhomogeneous interface to be identified by changing the input polarization direction, which alters the relative contribution of the tensor components to the overall NI MSHG response. In this paper, temperature-dependent magnetic contrast measurements of the capped Fe nanostripes are combined with loop measurements to provide evidence for two distinct magnetic contributions for 0.75 and 2.0 ML Fe coverages.

## II. EXPERIMENT

Preparation of the Au-capped ultrathin Fe films has been described in detail elsewhere.[25] Briefly, pseudomorphic Fe films were grown under ultrahigh-vacuum conditions (base pressure $< 4 \times 10^{-11}$ mbar) on a clean vicinal W(110) single-crystal substrate, offcut in the $[1\bar{1}0]$ ($x$) direction, which produces atomic steps running in the [001] ($y$) direction. This offcut was chosen to allow direct comparison with previous work by Elmers and co-workers.[11–16] The films were formed by deposition at room temperature followed by annealing at 800 K for 3 min. The Fe films were protected from *ex situ* contamination by a 16-nm-thick, optically isotropic capping layer of Au, deposited at room temperature. The capped samples were placed in an optical cryostat and the MSHG intensity, $I_y(2\omega;\varphi,M_X)$ (see below), was measured between 80 and 325 K with the applied magnetic field aligned along the easy axis. The $2\omega$ electric-field vector was aligned along the steps, and the input polarization angle $\varphi$ could be varied. A femtosecond laser system was used as the fundamental frequency light source, tuned to 1.5 eV.[10] Calculations predict a strong MSHG response from the Fe films in this spectral region.[26] Unamplified, 130 fs Ti:sapphire laser pulses of an average power of 0.9 W were used, at a repetition rate of 76 MHz. The beam size was 40 $\mu$m at the sample and the angle of incidence was $\leqslant 3^\circ$. Transient surface heating at the energy density used is less than 1 K,[27] and no change in the steady-state sample temperature was observed for these metallic samples on exposure to the laser beam.

## III. NI MSHG FROM MAGNETIC INTERFACES OF 1 M SYMMETRY

The third-rank *even* crystallographic tensor components and fourth-rank *odd* magnetic tensor components in Eq. (1) are expressed using the simplified notation $\chi_{ijk} = ijk$ and $\chi_{ijkL} = ijkL$, respectively, where the upper-case subscript $L$, describing the magnetization direction, is introduced to avoid potential confusion with unrelated quadrupolar susceptibility tensor components.[7] The interface formed by the pseudomorphic deposition of a magnetic species on a vicinal surface, consisting of well-ordered 1 m atomic steps separated by higher-symmetry surface terraces, possesses overall 1 m symmetry. If the surface normal of the interface is in the $z$ direction, the normal to the single mirror plane is in the $y$ direction, and the magnetization is in the $x$ direction, then the dependence of the $y$-polarized NI MSHG intensity on $\varphi$, the angle between the input polarization field and the $x$ direction, is given by[10]

$$I_y(2\omega,\varphi,\pm M_X) \propto |yxy \sin 2\varphi \pm \{yxxX \cos^2\varphi + yyyX \sin^2\varphi\} M_X|^2. \tag{2}$$

As well as producing these relatively simple expressions, NI geometry has the advantage of eliminating any isotropic capping layer contribution to the even term, and thus also to the phase difference. If the surface of the capping layer is macroscopically isotropic, as is often the case when no special effort is made to grow an epitaxial capping layer, then NI ensures no contribution to the *even* terms from the surface of the cap. Based on both theory and experiment, a typical value of $|ijkLM_L/i'j'k'|$ is 0.1.[10,19,28] Also, measuring the $y$-polarized NI MSHG intensity near $\varphi = 0^\circ$ or $\varphi = 90^\circ$ reduces the *odd* contribution effectively to a single tensor component, $yxxX$ or $yyyX$, respectively, simplifying the interpretation of results.

Buried magnetic interfaces are generally inhomogeneous, with distinct magnetic regions where the same magnetic species is found with different numbers of magnetic, substrate, and capping layer nearest neighbors. Both the magnetization[12,29] and the nonlinear optical susceptibility[30] in the interfacial region are known to depend sensitively on nearest-neighbor numbers and composition, requiring the contribution of the different regions to be included in the phenomenological model. This remains manageable for small numbers of distinct regions, particularly where the magnetic hysteresis loops are centrosymmetric. For such loops, further simplification of Eq. (2) is possible, using the type II procedure of McGilp *et al.*,[10,31]

$$\begin{aligned}\Delta I_y^{\pm}(2\omega;\varphi,H) &\equiv I^{\pm}(2\omega;\varphi,H) - I^{\mp}(2\omega;\varphi,-H) \\ &\propto 4\sin 2\varphi \cos^2\varphi \sum_{n,n'} |yxy^{(n)}||yxxX^{(n')}| \\ &\times \cos\left(\Delta\theta_{yx}^{nn'}\right) M_X^{\pm(n')} + 4\sin 2\varphi \sin^2\varphi \\ &\times \sum_{n,n'} |yxy^{(n)}||yyyX^{(n')}| \cos\left(\Delta\theta_{yy}^{nn'}\right) M_X^{\pm(n')},\end{aligned} \tag{3}$$

where $I^+$ refers to $H$ increasing from an initial negative value, and $I^-$ refers to $H$ decreasing from an initial positive value,

$\Delta\theta_{yi}^{nn'} = \theta_{yxy}^{n} - \theta_{yiiX}^{n'}$, where $\theta$ are the complex phase factors of the tensor components, and the sum is over the $n$ components contributing to the response, including cross-terms where $n \neq n'$. This procedure removes all terms even in the magnetization, in particular the quadratic contribution, the magnetoelastic terms, and the cross-terms in the magnetization from different components. Equation (3) shows explicitly that measuring the $y$-polarized NI MSHG intensity near $\varphi = 0^\circ$ or $\varphi = 90^\circ$, while limiting the *odd* contribution effectively to a single tensor component, $yxxX$ or $yyyX$, respectively, reduces the overall intensity substantially via the leading $\sin 2\varphi$ term. However, simulations confirm that such measurements maximize the probability of detecting contributions from different magnetic components.[9,10] It is also important to note that, in contrast to the magnetic terms, the crystallographic $yxy^{(n)}$ terms can only originate at the steps and edges, as the terrace contribution is forbidden by its 2 mm symmetry.

This much simplified equation can be fitted, for example, using normalized sigmoidal magnetization loops of the form

$$M^{(n)+}(H) = -1 + 2/\{1 + \exp[-s^{(n)}(H - H_c^{(n)})]\}, \quad (4)$$

where $s^{(n)}$ is the softness and $H_c^{(n)}$ the coercivity of the $n$th component. Only the magnetization depends on the applied magnetic field in Eq. (3), with the remaining terms determining the size of the measured response. In the absence of other information, this prevents the strength of the magnetization from being determined, but the softness and coercivity are unaffected by these scaling factors. In addition, the phase difference between the magnetic terms and the crystallographic $yxy$ component can be determined, and also the relative size of the two magnetic terms.

The full expression for the magnetic contrast or asymmetry is more complicated, but some simplification occurs for $\varphi$ close to $0^\circ$ and $90^\circ$ (and symmetry-related angles):

$$A_{\varphi\approx 0} \equiv \frac{I_y^+ - I_y^-}{I_y^+ + I_y^-} = \frac{4\varphi \sum_{n,n'} |yxy^{(n)}||yxxX^{(n')}| \cos\left(\Delta\theta_{xx}^{nn'}\right) M^{(n')}}{4\varphi^2 \sum_{n,n'} |yxy^{(n)}||yxy^{(n')}| \cos\left(\Delta\theta_{yxy}^{nn'}\right) + \sum_{n,n'} |yxxX^{(n)}||yxxX^{(n')}| \cos\left(\Delta\theta_{yxxX}^{nn'}\right) M^{(n)} M^{(n')}}, \quad (5)$$

$$A_{\varphi\approx \frac{\pi}{2}} = \frac{4\left(\frac{\pi}{2} - \varphi\right) \sum_{n,n'} |yxy^{(n)}||yyyX^{(n')}| \cos\left(\Delta\theta_{yy}^{nn'}\right) M^{(n')}}{4\left(\frac{\pi}{2} - \varphi\right)^2 \sum_{n,n'} |yxy^{n}||yxy^{(n')}| \cos\left(\Delta\theta_{yxy}^{nn'}\right) + \sum_{n,n'} |yyyX^{(n)}||yyyX^{(n')}| \cos\left(\Delta\theta_{yyyX}^{nn'}\right) M^{(n)} M^{(n')}}, \quad (6)$$

where $\Delta\theta_{yxy}^{nn'} = \theta_{yxy}^{n} - \theta_{yxy}^{n'}$, etc. The importance of the magnetic contrast is that it can be used to investigate temperature-dependent behavior if the variation of the tensor components with temperature is small over the temperature range of interest. Equation (3) can be used with Eq. (5) or (6) in a simultaneous fitting procedure that relies on a common set of tensor components.

Magnetoelastic terms can, in principle, contribute to the denominator in Eq. (5) or (6). However, such a contribution would also produce an acentric magnetization loop, which the use of type I extraction of McGilp *et al.*[10,31] would reveal. No evidence of a significant magnetoelastic contribution was found for this material system. Finally, the shape of a ferromagnetic transition in the $n$th magnetic component is approximated by a simple Fermi-type function of the form

$$M^{(n)}(T) = 1/\{1 + \exp[(T - T_c^{(n)})/\sigma^{(n)}]\}, \quad (7)$$

where $T_c^{(n)}$ is an effective Curie temperature, discussed in more detail below, and $\sigma^{(n)}$ measures the sharpness of the transition. The SNR for these measurements, using unamplified pulses, does not justify exploring critical behavior in the transition region in more detail.

## IV. RESULTS AND DISCUSSION

Iron deposition on vicinal W(110), and subsequent annealing, produces Fe nanostripes a single atom thick by self-assembly at the steps. The width of the stripes increases with further deposition until the (110) terraces are fully covered.[13] This growth mode continues to about 2 ML,[32] but, at higher coverage, Stranski-Krastanov growth occurs, with large Fe islands being formed at least ten atomic layers thick on a pseudomorphic Fe monolayer.[33] Capping such Fe stripes and layers with Au at room temperature does not produce any interdiffusion or reaction.[16]

The upper left panels of Figs. 1–3 show pairs of MSHG intensity data for $\varphi \approx 0^\circ$ and $\varphi \approx 90^\circ$, after type II extraction, from the 0.25, 0.75, and 2.0 ML Fe structures at 80 K, together with fits using Eqs. (3) and (4). The upper right panels show the temperature variation from 80 to 325 K, for $\varphi \approx 0^\circ$, of the MSHG contrast of the saturated magnetization, and the simultaneous fit using Eqs. (5)–(7). The lower panels show the extracted curves, in each case, while the parameter values, with estimated errors, are presented in Table I. All the figures show that it is possible to extract a common set of parameters by simultaneously fitting the loops measured at 80 K and the temperature-dependent magnetic contrast, confirming that any temperature dependence of the tensor components is not significant under these experimental conditions.

Only a single magnetic component can be identified from the 0.25 ML Fe data in Fig. 1. The data in Fig. 2, however, clearly show two identifiable components for the 0.75 ML Fe structure. In Fig. 3, the temperature dependence of the magnetic contrast indicates two components for the 2.0 ML Fe sample, and close inspection of the normalized hysteresis loops shows a small difference in the $\varphi \approx 0^\circ$ and $\varphi \approx 90^\circ$ response (Fig. 3, inset). Normalizing the extracted loops produces identical results where only a single component is contributing, as can be seen from Eq. (3). A good simultaneous fit to the data of Fig. 3 can only be obtained if it is assumed

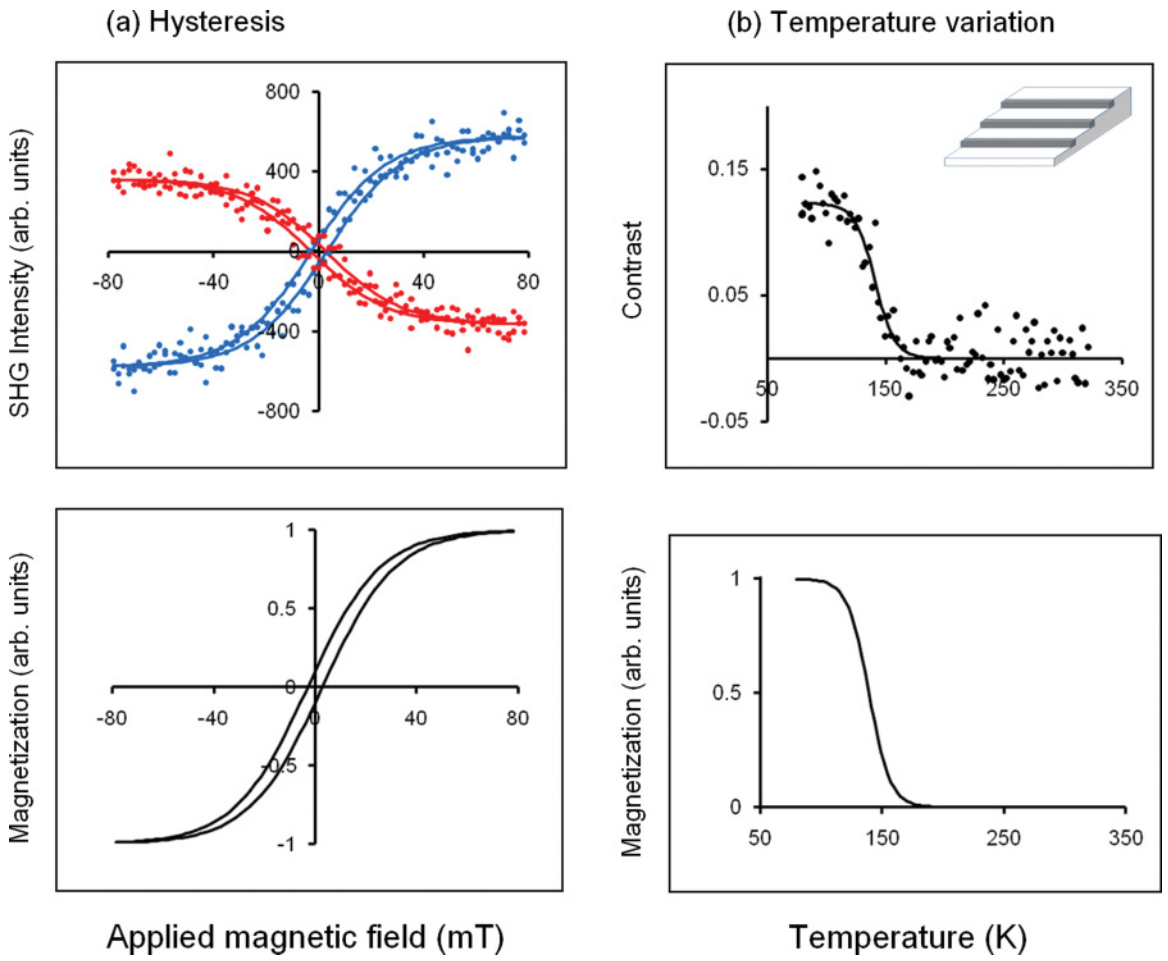


FIG. 1. (Color online) (a) NI MSHG $y$-polarized intensity difference, $\Delta I_y$, at 80 K and fits (solid lines), together with the resulting hysteresis curve (below), from Au-capped 0.25 ML Fe films grown on vicinal W(110): $\varphi \approx 0^\circ$ (●), $\varphi \approx 90^\circ$ (●). (b) Temperature variation of the MSHG contrast and simultaneous fit, together with extracted magnetization curve (below). Inset: schematic of 10-atom-wide Fe stripes grown out from the step edge (capping by Au not shown).

that two components are contributing to the MSHG response. Regarding the relative phases of the magnetic terms, values of greater than 90° are associated with the reversed loops of Figs. 1 and 2.[31] For the 0.75 ML Fe sample, this has the additional consequence that the coherent contributions of the magnetic components partially destructively interfere, and thus the contrast increases when this contribution is switched off above $T_c$ for the second component (Fig. 2, right column).

The Fe atoms in submonolayer stripes have three different nearest-neighbor arrangements, corresponding to Fe stripe atoms at the inner W step, at the outer edge of the stripe, and within the main terrace component of the stripe. For Fe stripes grown on a bcc (110) surface, a significant difference in the magnetic response is expected between the Fe atoms within the stripe, which have four Fe nearest neighbors, and the Fe atoms at the boundaries (step and edge) of the stripe, which have three Fe nearest neighbors.[10] Indeed,

TABLE I. Fitted values of the parameters for the three samples. The estimated error in the last figure is given in parentheses. The coercivity was measured at 80 K.

| | 0.25 ML Fe | 0.75 ML Fe | 0.75 ML Fe | 2.0 ML Fe | 2.0 ML Fe |
|---|---|---|---|---|---|
| | First component | First component | Second component | First component | Second component |
| $yxxX$ | $0.19(1)e^{i68(1)^\circ}$ | $0.03(1)e^{i140(3)^\circ}$ | $0.00(1)e^{i44(3)^\circ}$ | $2.67(2)e^{i34(1)^\circ}$ | $0.2(2)e^{i0(15)^\circ}$ |
| $yyyX$ | $0.17(1)e^{i102(1)^\circ}$ | $0.12(1)e^{i57(1)^\circ}$ | $0.16(1)e^{i81(1)^\circ}$ | $0.10(1)e^{i84(1)^\circ}$ | $0.018(2)e^{i38(5)^\circ}$ |
| $H_c$ (mT) | 3(1) | 24(1) | 7(2) | 30(1) | 20(1) |
| $s$ ($mT^{-1}$) | 0.07(1) | 0.05(1) | 0.04(1) | 0.6(1) | 0.2(1) |
| $T_c$ (K) | 140(10) | 202(3) | 141(5) | 274(4) | 160(10) |
| $\sigma$ (K) | 9(5) | 19(2) | 17(3) | 14(4) | 10(10) |

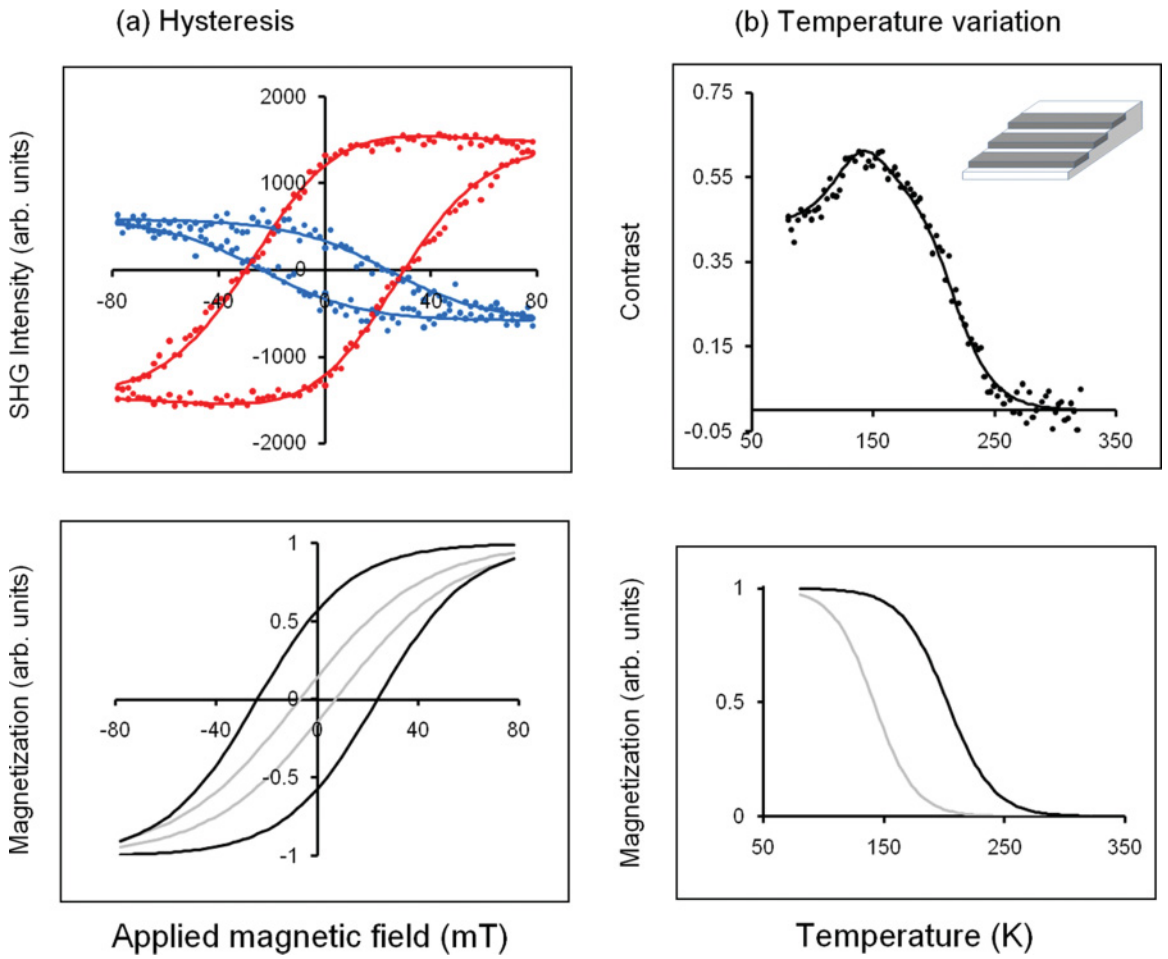


FIG. 2. (Color online) (a) NI MSHG $y$-polarized intensity difference, $\Delta I_y$, at 80 K and fits (solid lines), together with the resulting hysteresis curve (below), from Au-capped 0.75 ML Fe films grown on vicinal W(110): $\varphi \approx 0^\circ$ (●), $\varphi \approx 90^\circ$ (●). (b) Temperature variation of the MSHG contrast and simultaneous fit, together with extracted magnetization curves (below). Inset: schematic of 30-atom-wide Fe stripes grown out from the step edge (capping by Au not shown).

magneto-optic Kerr effect (MOKE) studies of ferromagnetic films grown on vicinal and curved substrates showed that the presence of steps can induce an in-plane uniaxial anisotropy,[2] and that the dependence of the step-induced anisotropy strength on step density was consistent with a nearest-neighbor Néel pair-bonding model.[34,35] A second example is the magnetic anisotropy of two-dimensional, submonolayer Co islands grown on Pt(111), which has been shown to be principally determined by the edge atoms, whose orbital moment is less quenched because of their reduced coordination.[36]

Figures 2 and 3 show that two magnetic contributions can be identified for two of the samples. Table I gives $T_c$ values that can be compared with a previous detailed MOKE study of this 1.4° vicinal W(110)/Fe system, capped with 6 ML Au.[16] Characteristic temperatures $T_s$ are given, which are the extrapolation to zero magnetization of the variation of the saturated magnetization with temperature. However, $T_s$ (or the effective $T_c$ used here) does not mark a critical phase transition in the spin block model of the stripes, which is discussed in more detail below. Equation (7) defines an effective $T_c$ value where the magnetization is reduced by 50%. Comparable $T_s$ values can be determined from the fitted curves in Figs. 1–3, where the contrast reduces to below 5%. $T_s$ values for the first component are 170(20) K for 0.25 ML, 260(10) K for 0.75 ML, and 315(10) K for 2.0 ML, which compares with 225(10) K for 0.3 ML, 250(10) K for 0.75 ML, and 295(10) K for 1 ML Fe, from figure 4 of Pratzer *et al.*,[16] with error estimates based on the scatter of the data. Given the approximations used in determining $T_s$, these results are in reasonable agreement, except for the 0.25 ML Fe value. In this region, the $T_s$ values are beginning to decline as coverage is reduced, so a slightly lower value is expected. The $H_c$ values of 7(2) and 24(1) mT at 80 K for the two components of the 0.75 ML Fe structure in Table I agree quite well with the published value of 30 mT for the single component observed by MOKE for 0.7 ML Fe at 111 K.[16] Previous MSHG work reported a higher value of $H_c$, which arose from the ambiguity in the relative sign of the phase of the two components that this temperature-dependent study removes.[10] The large temperature range over which the saturation magnetization reduces to zero is also consistent with the previous MOKE results.

The agreement of these data with previous MOKE results provides support for the analytical approach of the previous section. However, no direct evidence of a second component in the magnetic response at sub-ML coverage has been reported

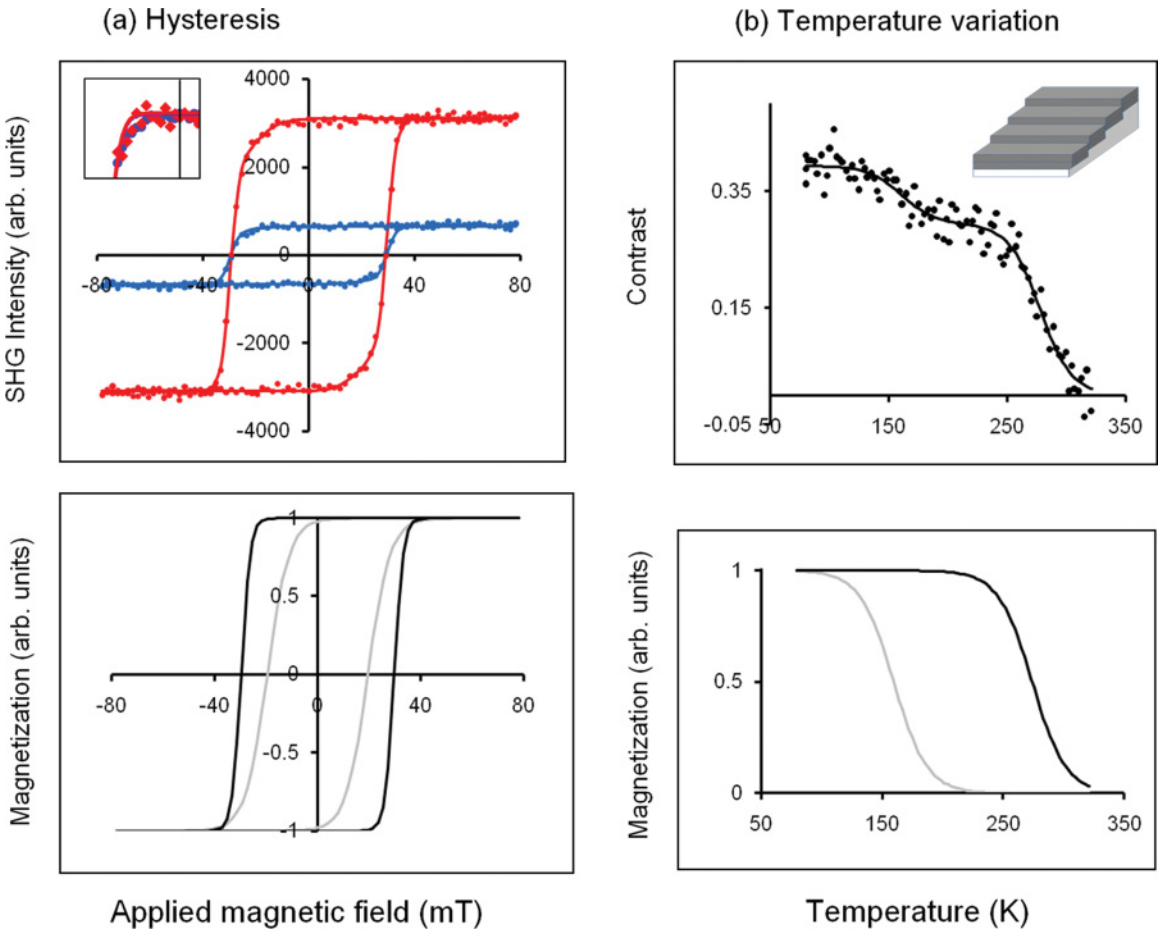


FIG. 3. (Color online) (a) NI MSHG $y$-polarized intensity difference, $\Delta I_y$, at 80 K and fits (solid lines), together with the resulting hysteresis curve (below), from Au-capped 2 ML Fe films grown on vicinal W(110): $\varphi \approx 0^\circ$ (●), $\varphi \approx 90^\circ$ (●). Inset: enlargement of normalized curves showing a small change in shape (b) Temperature variation of the MSHG contrast and simultaneous fit, together with extracted magnetization curves (below). Inset: schematic of 2 ML of Fe grown on the stepped W(110) substrate (capping by Au not shown).

in detailed MOKE studies.[15,16] MOKE measures the total response from the step, edge, and terrace atoms,[2] and, for this offcut and 0.75 ML coverage, boundary atoms will contribute only ∼5% of the signal. The MOKE response is expected to be dominated by the terrace magnetization for this low angle offcut at these coverages. In contrast, SHG can be disproportionately sensitive to step structure,[18] leading to the detection of boundary components of the magnetization.

Key evidence for this interpretation comes from the 2.0 ML Fe results in Fig. 3, where two components are identified. The Fe bilayer film nominally has two interfaces, W/Fe and Fe/Au, but calculations for Fe bilayers on W(110) show that the extended character of the electronic wave functions produces significant magnetic interactions extending three atomic layers into the substrate.[37] The Fe bilayer is part of a single interfacial region, in contrast to higher coverages, where Stranski-Krastanov growth of large Fe islands at least ten atomic layers thick allows distinct contributions from W/Fe and Fe/Au interfaces to be detected.[10] Ruderman-Kittel-Kasuya-Yosida (RKKY) indirect exchange coupling, mediated by the conduction electrons of the substrate or capping layer, must also be considered. However, it has been shown previously for this capped system that the effects of both dipolar and indirect exchange coupling between the stripes disappear, as expected, when the stripes overlap to form a contiguous film.[15] The much smaller size of the second component is consistent with a contribution from Fe atoms at the boundaries of the stripes, and the lower value of $T_c$ is expected, given the smaller number of exchange coupled neighbors of these boundary atoms.[38] The second component of the 0.75 ML sample also has a substantially lower value of $T_c$, consistent with this interpretation. Previous work has identified only a small RKKY lateral interaction at this coverage.[15] A plausible explanation of the absence of evidence for a second magnetic component in the 0.25 ML sample is that $T_c$ for this component is below 100 K and gives no measurable MSHG contribution in the accessible temperature range.

The MOKE results provide indirect evidence of step and edge effects, however. A significant boundary correction is required in the plots of interface energy versus stripe width used to determine the domain-wall energy. The data are collected above 160 K and are interpreted in terms of spin blocks behaving as single giant moments, which are temperature-dependent via the varying length of the spin block. The magnetization within the spin block is smaller than the

ground-state magnetization because of fluctuating single spins, particularly at the boundaries of the stripes, an interpretation supported by Monte Carlo simulations.[16] The most likely origin of the second MSHG component, which appears at much lower temperatures, is the boundary of the stripes, where the Fe atoms have fewer exchange-coupled nearest neighbors and different anisotropy energies compared to Fe atoms in the interior of the spin block. It is proposed that the spins are aligned at the boundaries below the lower characteristic temperature and that the alignment breaks up in a similar manner to that of the spin blocks as the temperature increases. Further experiments at lower temperatures and using amplified laser pulses should allow 5–30-atom-wide stripes to be explored in more detail. The use of different vicinal offcuts would also allow the RKKY lateral indirect exchange interactions in this coverage regime to be studied systematically.

## V. CONCLUSION

MSHG offers the important diagnostic capability of exploiting the properties of the optical tensor components to identify different magnetization contributions from inhomogeneous interface structures, because the tensor components vary with the local atomic structure. Temperature-dependent MSHG studies of Fe nanostripes grown on vicinal W(110), capped with Au, have confirmed the presence of two components in the magnetic response from the Fe stripes at 0.75 ML coverage and the Fe bilayer at 2.0 ML coverage. Comparison with previous work leads to the conclusion that, in this temperature régime, the lower temperature component arises from spin alignment at the boundaries of spin blocks. The behavior of boundary spins such as these is expected to be important for atomic-scale magnetic structures, such as Co atomic wires grown on Pt(997).[39,40]

## ACKNOWLEDGMENTS

The authors acknowledge the financial support of Science Foundation Ireland (SFI) provided under Contract No. 05/RFP/PHY030, and the Irish Research Council for Science, Engineering and Technology (IRCSET). Useful discussions with Dr. Mauro Ferreira and Professor Michael Coey are acknowledged.

*jmcgilp@tcd.ie

[1] F. Himpsel, J. Ortega, G. Mankey, and R. Willis, Adv. Phys. **47**, 511 (1998).
[2] S. Bader, Surf. Sci. **500**, 172 (2002).
[3] W. Weber, D. Kerkmann, D. Pescia, D. A. Wesner, and G. Guntherodt, Phys. Rev. Lett. **65**, 2058 (1990).
[4] J. Bartolome, L. M. Garcia, F. Bartolome, F. Luis, R. Lopez-Ruiz, F. Petroff, C. Deranlot, F. Wilhelm, A. Rogalev, P. Bencok, N. B. Brookes, L. Ruiz, and J. M. Gonzalez-Calbet, Phys. Rev. B **77**, 184420 (2008).
[5] J. McGilp, J. Phys. Condens. Matter **2**, 7985 (1990).
[6] J. McGilp, J. Phys. Condens. Matter **22**, 084018 (2010).
[7] A. Kirilyuk and T. Rasing, J. Opt. Soc. Am. B **22**, 148 (2005).
[8] L. Sampaio, A. Mougin, J. Ferre, P. Georges, A. Brun, H. Bernas, S. Poppe, T. Mewes, J. Fassbender, and B. Hillebrands, Europhys. Lett. **63**, 819 (2003).
[9] L. Carroll, K. Fleischer, and J. McGilp, Phys. Status Solidi C **5**, 2645 (2008).
[10] L. Carroll, K. Fleischer, J. Cunniffe, and J. McGilp, J. Phys. Condens. Matter **20**, 265002 (2008).
[11] H. J. Elmers, J. Hauschild, H. Hoche, U. Gradmann, H. Bethge, D. Heuer, and U. Kohler, Phys. Rev. Lett. **73**, 898 (1994).
[12] H. Elmers, Int. J. Mod. Phys. B **9**, 3115 (1995).
[13] J. Hauschild, H. J. Elmers, and U. Gradmann, Phys. Rev. B **57**, 677 (1998).
[14] M. Pratzer, H. J. Elmers, M. Bode, O. Pietzsch, A. Kubetzka, and R. Wiesendanger, Phys. Rev. Lett. **87**, 127201 (2001).
[15] M. Pratzer and H. J. Elmers, Phys. Rev. B **66**, 033402 (2002).
[16] M. Pratzer and H. J. Elmers, Phys. Rev. B **67**, 94416 (2003).
[17] P. Gambardella, A. Dallmeyer, K. Maiti, M. Malagoli, W. Eberhardt, K. Kern, and C. Carbone, Nature (London) **416**, 301 (2002).
[18] J. R. Power, J. D. O'Mahony, S. Chandola, and J. F. McGilp, Phys. Rev. Lett. **75**, 1138 (1995).
[19] R. P. Pan, H. D. Wei, and Y. R. Shen, Phys. Rev. B **39**, 1229 (1989).
[20] J. W. Jeong, S. C. Shin, I. L. Lyubchanskii, and V. N. Varyukhin, Phys. Rev. B **62**, 13455 (2000).
[21] H. Callen and E. Callen, Phys. Rev. **132**, 991 (1963).
[22] E. du Tremolet de Lacheisserie, Phys. Rev. B **51**, 15925 (1995).
[23] Y. R. Shen, *The Principles of Non-linear Optics* (Wiley, New York, 1984).
[24] L. Carroll and J. McGilp, Phys. Status Solidi C **0**, 3046 (2003).
[25] K. Fleischer, L. Carroll, C. Smith, and J. McGilp, J. Phys. Condens. Matter **19**, 11 (2007).
[26] J. P. Dewitz, J. Chen, and W. Hubner, Phys. Rev. B **58**, 5093 (1998).
[27] J. I. Dadap, Z. Xu, X. F. Hu, M. C. Downer, N. M. Russell, J. G. Ekerdt, and O. A. Aktsipetrov, Phys. Rev. B **56**, 13367 (1997).
[28] W. Hubner and K. H. Bennemann, Phys. Rev. B **40**, 5973 (1989).
[29] D. Repetto, T. Y. Lee, S. Rusponi, J. Honolka, K. Kuhnke, V. Sessi, U. Starke, H. Brune, P. Gambardella, C. Carbone, A. Enders, and K. Kern, Phys. Rev. B **74**, 54408 (2006).
[30] Q. Y. Jin, H. Regensburger, R. Vollmer, and J. Kirschner, Phys. Rev. Lett. **80**, 4056 (1998).
[31] J. McGilp, L. Carroll, and K. Fleischer, J. Phys. Condens. Matter **19**, 396002 (2007).
[32] J. Hauschild, U. Gradmann, and H. Elmers, Appl. Phys. Lett. **72**, 3211 (1998).
[33] M. Bode, A. Wachowiak, J. Wiebe, A. Kubetzka, M. Morgenstern, and R. Wiesendanger, Appl. Phys. Lett. **84**, 948 (2004).
[34] R. K. Kawakami, E. J. Escorcia-Aparicio, and Z. Q. Qiu, Phys. Rev. Lett. **77**, 2570 (1996).
[35] E. J. Escorcia-Aparicio, H. J. Choi, R. K. Kawakami, and Z. Q. Qiu, Phys. Rev. B **58**, 93 (1998).

[36]P. Gambardella, S. Rusponi, T. Cren, N. Weiss, and H. Brune, Acad. Sci. Comp. Rend. Phys. **6**, 75 (2005).
[37]X. Qian and W. Hubner, Phys. Rev. B **60**, 16192 (1999).
[38]R. Skomski and J. Coey, *Permanent Magnetism* (Institute of Physics, Bristol, 1999).
[39]P. Gambardella, A. Dallmeyer, K. Maiti, M. C. Malagoli, S. Rusponi, P. Ohresser, W. Eberhardt, C. Carbone, and K. Kern, Phys. Rev. Lett. **93**, 077203 (2004).
[40]J. Cunniffe, D. McNally, M. Liberati, E. Arenholz, C. McGuinness, and J. McGilp, Phys. Status Solidi B **247**, 2108 (2010).